Generation of chordoma cell line JHC7 and the identification of Brachyury as a novel molecular target:

Laboratory investigation

Wesley Hsu, M.D.[1,*], **Ahmed Mohyeldin, Ph.D.**[1], **Sagar R. Shah, M.S.**[1,2], **Colette M. ap Rhys, Ph.D.**[1], **Lakesha F. Johnson, B.S.**[1], **Neda I. Sedora-Roman, M.D.**[1], **Thomas A. Kosztowski, M.D.**[1], **Ola A. Awad, Ph.D.**[4], **Edward F. McCarthy, M.D.**[3], **David M. Loeb, M.D., Ph.D.**[4], **Jean-Paul Wolinsky, M.D.**[1], **Ziya L. Gokaslan, M.D.**[1], and **Alfredo Quiñones-Hinojosa, M.D.**[1]

[1]Department of Neurosurgery and Oncology, Brain Tumor Stem Cell Laboratory, The Johns Hopkins University School of Medicine, Baltimore, Maryland [2]Department of Biomedical Engineering, The Johns Hopkins University School of Medicine, Baltimore, Maryland [3]Department of Pathology, The Johns Hopkins University School of Medicine, Baltimore, Maryland [4]Department of Oncology and Pediatrics, Musculoskeletal Tumor Program, The Johns Hopkins University School of Medicine, Baltimore, Maryland

Abstract

Object—Chordoma is a malignant bone neoplasm hypothesized to arise from notochordal remnants along the length of the neuraxis. Recent genomic investigation of chordomas has identified *T* (Brachyury) gene duplication as a major susceptibility mutation in familial chordomas. Brachyury plays a vital role during embryonic development of the notochord and has recently been shown to regulate epithelial-to-mesenchymal transition in epithelial-derived cancers. However, current understanding of the role of this transcription factor in chordoma is limited due to the lack of availability of a fully characterized chordoma cell line expressing Brachyury. Thus, the objective of this study was to establish the first fully characterized primary chordoma cell line expressing gain of the *T* gene locus that readily recapitulates the original parental tumor phenotype in vitro and in vivo.

Methods—Using an intraoperatively obtained tumor sample from a 61-year-old woman with primary sacral chordoma, a chordoma cell line (JHC7, or Johns Hopkins Chordoma Line 7) was

established. Molecular characterization of the primary tumor and cell line was conducted using standard immunostaining and Western blotting. Chromosomal aberrations and genomic amplification of the *T* gene in this cell line were determined. Using this cell line, a xenograft model was established and the histopathological analysis of the tumor was performed. Silencing of Brachyury and changes in gene expression were assessed.

Results—The authors report, for the first time, the successful establishment of a chordoma cell line (JHC7) from a patient with pathologically confirmed sacral chordoma. This cell line readily forms tumors in immunodeficient mice that recapitulate the parental tumor phenotype with conserved histological features consistent with the parental tumor. Furthermore, it is demonstrated for the first time that silencing of Brachyury using short hairpin RNA renders the morphology of chordoma cells to a more differentiated-like state and leads to complete growth arrest and senescence with an inability to be passaged serially in vitro.

Conclusions—This report represents the first xenograft model of a sacral chordoma line described in the literature and the first cell line established with stable Brachyury expression. The authors propose that Brachyury is an attractive therapeutic target in chordoma and that JHC7 will serve as a clinically relevant model for the study of this disease.

Keywords

Chordomas are tumors that predominantly arise from the osseous spine and skull base, comprise 2%–4% of all bone cancers, and are often refractory to treatment, with a median survival of approximately 6 years.[13] Recent reports on the incidence and survival patterns of patients with chordomas underscore the dismal prognosis of this disease with long-term survival rates at 5, 10, and 20 years precipitously dropping to 67%, 40%, and 13%, respectively.[13] Chordomas are often difficult to manage given their locally destructive behavior and predilection to grow near critical skull base and lumbosacral nerves as well as blood vessels.[6,10–12,36] The invasive nature of this cancer makes complete resection impossible in 50% of the cases of sacral chordomas and even more difficult in the mobile spine and skull base.[1] In addition to such clinical challenges, breakthroughs in medical therapy for this disease continue to be delayed in part because of our poor understanding of its pathogenesis and lack of model systems to study it. Unlike other bone sarcomas that have established in vitro cell lines and xenograft models,[18,26,28,35] there has been little progress in these areas for chordoma. The paucity of cultured chordoma cell lines and lack of their complete characterization has delayed in vitro and in vivo investigation of this cancer.[4,16,20,23,32]

Chordomas are believed to derive from cranial and sacral vestiges of the human notochord, a mesoderm-derived embryonic structure that is critical for neurulation and embryonic tissue organization.[3,21,22,29,31] In vertebrates, it is replaced by the vertebral column to become the main axial support of the body. Microarray data from a broad range of connective tissue neoplasms indicate that, at the transcriptional level, chordomas express many genes known to be involved in cartilage development that uniquely distinguish them from other chondroid neoplasms. [15,29] A possible explanation for this unique transcriptome may come from the

recent implication of the embryonic transcription factor, Brachyury, found to be highly expressed by chordomas.[14,15,27,29,34] Brachyury is a T-box transcription factor known classically for its role in early embryonic gastrulation events and notochord development. [24] A study of 8 families with heritable chordoma found that duplications of the *T* (Brachyury) gene confer a major susceptibility to this malignancy.[34] Furthermore, Brachyury is expressed in embryonic notochord,[29] is essential for notochordal development,[7] and has been shown to be critical for morphogenetic migration of mesodermal cells during gastrulation.[8,19,30] Screening of Brachyury expression in chordoma revealed positive expression in 90% of all pathologically confirmed chordomas screened.[15] More recently, a role for Brachyury in cancer biology has been proposed.[5] Brachyury is found to be overexpressed in several epithelial cancers and promotes epithelial-to-mesenchymal transition by regulating the expression of E-cadherin and the mesenchymal transcription factor Slug.[5] Forced overexpression of Brachyury in human carcinoma cells upregulates mesenchymal stem cell markers, downregulates epithelial markers, and increases cell invasion, inducing changes consistent with epithelial-to-mesenchymal transition.[5] These findings collectively suggest a compelling role for Brachyury in the transformation of notochordal remnants and progression of chordoma.

Using tumor specimens obtained intraoperatively, we aimed to establish a chordoma cell line that accurately represented the human disease and that expressed stable levels of Brachyury with serial passaging. Previous studies aimed to establish chordoma cell lines failed to characterize the expression of Brachyury in the lines reported[16,20,23,32] or showed instability of Brachyury expression in vitro with serial passaging.[4] Only 1 study formally tested the tumor-forming capacity of chordoma cells in vivo, and this line was established from an extraaxial chordoma that showed unstable Brachyury expression in vitro when the cell line was passaged.[4] In this paper, we report for the first time the successful establishment of a chordoma cell line (JHC7) from a patient with pathologically confirmed sacral chordoma. This cell line readily forms tumors in immunodeficient mice that recapitulate the parental tumor phenotype with conserved histological features consistent with the parental tumor.

Furthermore, several studies attempting to identify novel therapeutic strategies have targeted chordoma growth by using inhibitors of signal transducers and activators of transcription 3 (STAT3)[33] as well as drugs that antagonize tyrosine kinases, such as imatinib mesylate (Gleevec, Novartis).[2,25] We propose that inhibition of Brachyury, a transcription factor that is silenced once notochord development is complete,[29] is a more attractive therapeutic target due to its tissue-specific expression observed only in neoplastic cells.[5,17] In addition, Brachyury regulates mesodermal cell migration developmentally[8,19,30] and promotes epithelial-to-mesenchymal transition in epithelial neoplasms, making it a compelling molecular target in cancer biology.[5] We demonstrate for the first time that silencing of Brachyury using shRNA renders the morphology of chordoma cells to a more differentiated-like state and leads to complete growth arrest with senescence and an inability to be passaged serially in vitro. Using this unique cell line, we have developed a novel xenograft model for chordoma in immunodeficient mice. This report represents the first xenograft

model of a sacral chordoma line described in the literature and the first cell line established with stable Brachyury expression.

Methods

Pathological Diagnosis

An intraoperatively obtained tumor sample from a 61-year-old woman with primary sacral chordoma and no previous history or treatment for oncological disease was diagnosed as classic chordoma based on clinical presentation, MR imaging, tissue histology, and immunostaining (S100β, cytokeratin [AE1/AE3], and Brachyury immunohistochemistry). Tissue was collected with consent from the patient under Johns Hopkins Institutional Review Board guidelines.

Establishment of Chordoma Cell Line

The tumor specimen was transported on ice directly from the operating room in calcium- and magnesium-free Hanks' balanced salt solution buffer. Dead, necrotic, and fibrous tissue was dissected out using forceps and a scalpel. Remaining tissue was transferred to a glass dish with 0.25% trypsin (Invitrogen) and cut into small fine pieces less than 0.5 cm in size with a scalpel. After fine cutting for 5–10 minutes, tissue was transferred to a sterile 15-ml tube (BD Falcon) and further dissociated into single cells by placing on a shaker for 20–30 minutes at 37°C. Digested tissue was further mechanically disassociated by adding DMEM/F12 with 10% FBS to stop enzymatic digestion and triturated using a 5-ml cell culture pipette tip until pieces of tissue and cells were able to be pipetted using a fire-polished Pasteur pipette. Once the tissue was thoroughly dissociated and readily passed through the tip of a Pasteur pipette, aggregates and cells were spun down and resuspended in fresh serum media (10% FBS in DMEM/F12; Invitrogen). This suspension was passed through a 40-μm nylon mesh filter (BD Falcon), and all single cells were collected and plated in 1 well of a 6-well plate. Twenty-four hours later debris and dead cells were aspirated and fresh media was added to adherent cells. Once this well reached confluency, it was passaged to a T-25 cm^2 adherent cell culture flask (BD Falcon) for expansion. Chordoma cells (JHC7 line) were maintained in serum media (10% FBS in DMEM/F12; Invitrogen) with antibiotic/antimycotic (Ab/Am, Invitrogen). Once the line was established, cell passing was maintained at 1:3 in DMEM/F12 with 10% FBS.

Immunostaining

Immunohistochemical assays were performed on formalin-fixed, paraffin-embedded human chordoma samples. Sections 10-μm thick were cut and all sections were deparaffinized with xylene and graded alcohols. For S100β and cytokeratin (AE1/AE3), the automated slide-staining system Benchmark XT (Ventana) was used for immunostaining. Cell Condition 1 buffer (Ventana) was used for antigen retrieval for S100β, and Protease 1 (Ventana) enzymatic digestion was used for antigen retrieval for AE1/AE3. Prediluted antibodies for S100β (Ventana) and AE1/AE3 (Ventana) were used for primary antibody incubation for 16 minutes. Prediluted biotinylated anti–mouse secondary antibodies (Ventana) and streptavidin-conjugated HRP (Ventana) were used to detect primary antibodies. The chromogen DAB was used to visualize immunoreactivity. For Brachyury immunostaining,

antigen retrieval was performed in a water bath at 95°C using sodium citrate (10 mM) for 30 minutes. Endogenous peroxidase activity was blocked with 0.3% H_2O_2 and 0.5% normal donkey serum in PBS. Cells were incubated overnight at 4°C with anti-Brachyury antibody (C-19) at a dilution of 1:50 in PBS with 0.3% Triton X-100 and 2% normal donkey serum. Immunoreactivity was visualized using biotinylated anti–goat secondary antibodies, streptavidin-HRP (BD Biosciences), and DAB (Sigma). For immunocytochemistry, cells were washed in cold PBS and fixed with 10% formalin in 35-mm cell culture plates (Corning). Cells were blocked with 10% normal donkey serum and incubated overnight at 4°C with anti-Brachyury antibody (C-19) at 1:50 in PBS with 0.3% Triton X-100 and 2% normal donkey serum. After washing with cold PBS, the primary antibody was detected using appropriate anti–goat secondary antibody (Molecular Probes, Invitrogen) conjugated with a fluorochrome. Nuclei were counterstained with DAPI or hematoxylin, based on the application.

Western Blotting

Chordoma tissue from the operating room or from xenografts was flash frozen in liquid nitrogen and then lysed using T-PER (Pierce) tissue extraction reagent. The JHC7 cells were lysed using radioimmunoprecipitation assay lysis buffer (Pierce). Protein concentrations were quantified using Bradford Dye Reagent (BioRad) and Western blots were performed by running 50 μg of whole cell lysate on 10% Bis-Tris NuPage gels (Invitrogen) and were transferred to polyvinylidene fluoride membranes (BioRad). Membranes were blocked with TBS/Tween with 5% nonfat dry milk (BioRad) overnight at 4°C and subsequently incubated at room temperature for 1 hour with Brachyury antibody, 1:300 (C-19, Santa Cruz). Immunoreactive bands were visualized using horseradish peroxidase-conjugated anti–goat antibodies (Pierce). Bands were detected using enhanced chemiluminescence reagent (Amersham).

Genomic DNA Extraction, DNA PCR, and Copy Number Analysis

A DNeasy Blood & Tissue Kit (Qiagen) was used for total genomic DNA isolation. Copy number quantification was performed using SYBR green and Applied Biosystem's 7300 Cycler.

Brachyury-specific DNA primer pair spanning a portion of both exonic and intronic regions of the *T* gene amplification site was used. A commercially obtained human mesenchymal stem cell line–derived genomic DNA was used to quantify amplification of the *T* gene in the JHC7 cell line. Glyceraldehyde 3-phosphate dehydrogenase was applied as an internal loading control. The following primer pairs were used: *T* gene, 5′-CAAAGCCCGGCCAAATGCGCT-3′ (forward) and 3′-AGCCTGCGATGCTCCCTGATTCCC-5′ (reverse); *GAPDH* gene, 5′-AATTGAGCCCGCAGCCTCCC-3′ (forward) and 5′-TCGGCTGGCGACGCAAAAGA-3′ (reverse).

RNA Extraction and Quantitative Real-Time PCR

Total RNA was extracted using TRIzol followed by phase separation using chloroform and was precipitated overnight at 4°C using isopropanol. Further isolation of total RNA was

performed using the RNeasy Mini Kit (Qiagen). Reverse transcription of purified RNA was performed using the Superscript III First-Strand cDNA Synthesis Kit (Invitrogen). Real-time PCR using SYBR Green (Applied Biosystems) and data analysis was performed on Applied Biosystem's 7300 Cycler. Glyceraldehyde 3-phosphate dehydrogenase was applied as an internal control. The following primer pairs were designed based on Harvard Primer Bank Guidelines (http://pga.mgh.harvard.edu/primerbank): *CDH1* gene (E-cadherin), 5′-CCCACCACGTACAAGGGTC-3′ (forward) and 5′-ATGCCATCGTTGTTCACTGGA-3′ (reverse); *CDH2* gene (N-cadherin), 5′-CAGATAGCCCGGTTTCATTTGA-3′ (forward) and 5′-CAGGCTTTGATCCCTCAGGAA-3′ (reverse); *Slug* gene, 5′-ATATTCGGACCCACACATTACCT-3′ (forward) and 3′-GCAAATGCTCTGTTGCAGTGA-5′ (reverse); and *GAPDH* gene, 5′-CATGAGAAGTATGACAACAGCCT-3′ (forward) and 3′-AGTCCTTCCACGATACCAAAGT-5′ (reverse).

Karyotyping

Semiconfluent cells were exposed to colcemide (0.15 μg/ml) for 24 hours. The cells were harvested and slides with metaphase spreads were prepared according to standard techniques. Chromosome aberrations were described using the International System of Human No-menclature.

Animal Xenografts

Nonobese diabetic/severe combined immunodeficient mice (NCI) were housed in a pathogen-free room controlled for temperature and humidity. Mice were manually immobilized in a prone position. Using a 23-gauge syringe, animals were injected subcutaneously with cultured chordoma cells in 25 μl of PBS at escalating cell counts of 500,000, 1 million, or 2 million cells. Animals were housed in standard facilities, given free access to water and rodent chow, and monitored periodically for tumor formation. All animals were treated in accordance with the policies and principles of laboratory animal care of the Johns Hopkins University School of Medicine Animal Care and Use Committee.

Histopathological Analysis

Animals were anesthetized at 4 months after injection and after visual confirmation of subcutaneous tumor formation. Tumors were harvested under sterile conditions and prepared for histopathological analysis by fixing tissues with 10% formalin. Specimens were embedded in paraffin, and 10-μm-thick sections were collected for H & E staining and processed further for immunostaining.

Lentiviral Transduction

A Mission TRC-Hs (Human) clone set of sequence-verified shRNA lentiviral plasmid vectors targeting Brachyury, TRCN0000005480–81, was obtained from the Johns Hopkins University High Throughput Biology Center. Vesicular stomatitis virus glycoprotein-pseudotyped virus was produced by cotransfecting 293T cells with an shRNA transducing vector and 2 packaging vectors, psPAX2 and pMD2.G, using Lipofectamine 2000. Infectious virus was harvested at 36 and 48 hours after transfection and filtered through a

0.22-μm pore size cellulose acetate filter. The virus was concentrated by centrifuging through a Millipore Centricon Plus-70. The JHC7 chordoma cells were transduced with concentrated virus supplemented with 5 μg/ml polybrene (Sigma). Twenty-four hours after transduction, cells were selected with 2.5-μg/ml puromycin (Sigma) and switched to 1.0 μg/ml after 3 days. Cells were harvested for further analysis after 10 days posttransduction. Empty vector JHC7 controls are referred to in this paper as "Control shRNA" while JHC7 cells that received Brachyury shRNA are referred to as "Brachyury shRNA."

MTT Assay

Five wells in a 96-well plate were seeded at 3000 cells/well. Four independent plates represented 4 independent time points (Days 5, 10, 15, and 20). Monotetrazolium (MTT, Sigma) was suspended at a concentration of 10 mg/ml in PBS (MTT solution). Twenty microliters of MTT solution was added to each well with 200 μl of fresh media, and the plate was incubated at 37°C for 4 hours in the dark. After 4 hours, each well was aspirated and the formazan salt was solubilized using 200 μl of isopropyl alcohol. Optical density measurements were read using a spectrophotometric plate reader (BioTek) at 570 nm. Optical density measurements from wells with no cells but with media and MTT solution only were used to measure background optical density. Measurements were taken at different cell seeding concentrations and at different time points for growth curve analysis. For control shRNA and Brachyury shRNA experiments, growth curve studies were performed 10 days after transduction where morphological phenotype differences were most prominent.

Cell Viability and Average Cell Diameter

Cell viability was assessed with trypan blue using the Vi-Cell XR Cell Viability Analyzer (Beckman Coulter). Ten days after transduction and antibiotic selection, cells were trypsinized and replated at 850,000 cells in T-25 cm^2 flasks. Cells were allowed to grow for 25 days under antibiotic cell selection, and on Day 25 both floating and attached cells were harvested after trypsinization and assessed for viability in triplicate with trypan blue using the Vi-Cell XR Viability Analyzer. In addition, average cell diameter was also analyzed during the same experiment using the Vi-Cell XR Viability Analyzer. Control shRNA and Brachyury shRNA cell groups were compared for percentage cell viability and average cell diameter.

Statistical Analysis

Data from experiments evaluating multiple time points were analyzed by ANOVA. Paired data were analyzed by Student t-tests. All statistical tests were 2-sided at the 5% level of significance.

Results

Pathological Confirmation of Chordoma Diagnosis

Intraoperatively obtained tissue from a 61-year-old woman with suspected chordoma presenting in the sacral spine was evaluated pathologically for features of chordoma. A sacral mass characteristic of chordoma was revealed on T1-weighted MR images (Fig. 1a

left). Staining of the original tumor using H & E revealed pathological features consistent with classical chordoma with some undifferentiated features. Histological examination revealed a lobulated tumor composed of cells separated by fibrous septa (Fig. 1a center and right). The cells have small round nuclei with abundant large vacuolations present within the cytoplasm (Fig. 1a center and right). Large vacuoles in the cytoplasm can be observed in the sample, giving the appearance of bubbles, a previously described distinguishing feature of classical chordoma often referred to in the literature as physaliferous features.[9] Accurate diagnosis of this sample was further evaluated using 3 markers (S100β, cytokeratin, and Brachyury) that, when used in combination, are pathognomonic for chordoma. Immunostaining was positive for all 3 markers as indicated by the formation of brown DAB chromogen product (Fig. 1b). The S100β and Brachyury markers demonstrated prominent nuclear expression consistent with their cellular localization noted in other cell types and tissues (Fig. 1b left and right). Cytokeratin staining revealed prominent cytoplasmic expression in all tumor cells consistent with previous reports on chordomas (Fig. 1b center). Furthermore, protein lysates from the primary chordoma sample revealed a 49 kD immunoreactive band consistent with the molecular weight for Brachyury as demonstrated with Western blotting (Fig. 1c).

Establishment and Characterization of Novel Chordoma Cell Line JHC7

Using the intraoperatively obtained chordoma tissue, a novel chordoma cell line was created (JHC7). Cultured cells were morphologically identical to classical chordoma, including the characteristic physaliferous phenotype that distinguishes this neoplasm (Fig. 2a). Phase contrast images for chordoma cells at the seventh passage demonstrated round cells with small nuclei and cytoplasm filled with small and large vacuoles (Fig. 2a). Cells appeared to make multiple cell-to-cell contacts, with small processes extending from one cell membrane to another cell membrane. The presence of Brachyury was confirmed by Western blotting and immunocytochemical analyses (Fig. 2a and c). Brachyury expression was clearly confined to the nucleus in all cells in culture, consistent with its role as a transcription factor (Fig. 2a). This observation is supported by nuclear localization of Brachyury expression that coincided with the DAPI signal, which counterstained nuclei in overlay images (Fig. 2a). These features of the chordoma phenotype were preserved over serial passages (approximately 15 by the time of this publication).

Consistent with the slow growth rate of chordoma in vivo, the JHC7 cell line demonstrated a slow doubling time consistent with the neoplasm's behavior (Fig. 2b). The MTT assay was used as an index for cell viability and proliferation. Reduction in MTT resulting in the formation of the insoluble formazan salt by escalating numbers of JHC7 cells reveals that doubling the cell number in vitro is roughly equivalent to a doubling in optical density measurements (data not shown). This suggests that optical density measurements may serve as a reliable indicator of doubling time in growth kinetic studies of JHC7 cells. For growth kinetic studies, cells demonstrated a doubling time of approximately 5 days (Fig. 2b). In addition, Brachyury expression in JHC7 cells was stable over serial passages in vitro as immunoreactive bands for Brachyury were prominent and consistent in intensity from cells harvested at the 4th, 10th, and 15th passages (Fig. 2c). Comparison of *T* gene copy number

using DNA PCR revealed that the JHC7 line harbors at least more than 1 genomic copy of the *T* gene when compared with normal human mesenchymal stem cells (Fig. 2d).

Cytogenetic analysis of G-banded chromosomes identified both numerical and structural clonal abnormalities. The composite karyotype for the analyzed 19 metaphases was as follows: 40~42,XX,−1,der(3)t(3;22) (q11.2;q11.2),−7,der(9)t(7;9)(q11.2;p13), −10,der(14)t(1;14) (q21;q22),−15,−16,der(17)t(7;17)(p13;p11.2),−21,−22,−22, +mar1 × 3,+mar2 [cp19] (Fig. 2e).

Subcutaneous Injection of Chordoma Cells Results and Tumor Formation

To investigate whether cultured chordoma cells are able to recapitulate the essential phenotypic characteristics of the parent tumor and to develop an animal model for further study of this disease, we subcutaneously injected these cells into nonobese diabetic/severe combined immunodeficient mice. Mice injected with chordoma cells formed tumors within 3–4 months after implantation at the initial site of injection (Fig. 3a). All animals injected with 2 million, 1 million, and 500,000 sixth-passage JHC7 cells formed tumors at the injected site (Fig. 3a). Representative tumors from an animal injected with 500,000 cells were well encapsulated and grossly resembled chordoma with gray-white complexion and lobulated appearance (Fig. 3a). As in the case with the parent tumor, Western blotting and immunostaining revealed that these tumors expressed Brachyury (Fig. 3b and c). Lysates from the native JHC7 line (Passage 7), the original tumor, and chordoma xenograft all revealed prominent expression of Brachyury at 49 kD (Fig. 3b). Gross and histological examination of xenografts revealed a lobulated tumor composed of cells separated by fibrous septa like the parent tumor (Fig. 3c). Histologically, these tumors resembled the parent tumor and possessed physaliferous features characteristic of chordoma (Fig. 3c). The cells of xenograft tumors had small round nuclei with abundant large vacuolations present within the cytoplasm, and all cells expressed Brachyury that localized to the nucleus (Fig. 3c).

Loss of Brachyury, Phenotypic Changes, and Loss of Proliferation

To investigate the role of Brachyury in cultured chordoma cells, JHC7 cells were transduced with 5 different shRNA vectors against Brachyury that showed either partial or complete knockdown (data not shown). Western blot analysis confirmed the loss of Brachyury expression in knockdown cells with the most efficient protein silencing (Fig. 4a). Loss of Brachyury abolished the classic phenotype of chordoma cells including physaliferous features and led to a more differentiated-like state with stellate-appearing cells (Fig. 4b). Using MTT assay as an index of proliferation, complete loss of proliferation capacity was observed in Brachyury shRNA JHC7 cells over a 37-day period when compared with control shRNA (empty vector; Fig. 4c). Serial passaging did not yield viable cell cultures of Brachyury shRNA cells when compared with control shRNA cells (data not shown). Cell viability was significantly compromised with a 20%–25% reduction in viability as measured by trypan blue exclusion (Fig. 4d). Brachyury knockdown cells demonstrated a significant decrease in average cell diameter size with nearly complete loss of cytoplasmic vacuoles (Fig. 4b and e). Consistent with a more differentiated morphological phenotype, loss of Brachyury resulted in minimal change of the baseline epithelial marker E-cadherin, but a

significant decrease in mesenchymal markers N-cadherin and the epithelial-to-mesenchymal transcriptional regulator Slug (Fig. 4f).

Discussion

Resection of chordoma, currently the gold standard of treatment, is often impossible to perform without damaging adjacent anatomical structures and causing significant clinical morbidity. Yet despite the most aggressive surgical approaches and advanced postoperative radiotherapy, recurrence is common. Advances in the development of adjuvant therapies for chordoma are limited due to the lack of fully characterized model systems that accurately recapitulate chordoma in vitro and in vivo. The evaluation of novel therapeutic drug strategies for chordoma has been limited to in vitro studies using available cell lines that have not been fully characterized for Brachyury expression or tumor initiating capacity.[16,20,23,32]

In this study, we report the derivation and full characterization of a primary chordoma cell line expressing Brachyury from a sacral tumor with verified tumor-initiating capacity and harboring a gain of the *T* gene locus. Pathological diagnosis of chordoma was confirmed based on clinical presentation, imaging, and rigorous histological criteria. Recent studies report that evaluation of cytokeratin when combined with Brachyury expression improves sensitivity and specificity for detection of chordoma by 98% and 100%, respectively.[15] Analysis of our tumor sample was pathologically confirmed as chordoma based on all of the above mentioned criteria including S100β staining, a marker often expressed by chordoma as well as characteristic physaliferous features on H & E staining (Fig. 1). Unlike previously described chordoma cell lines,[4,16,20,23,32] stable expression of Brachyury and classical phenotypic features of chordoma cells are maintained through serial passages in the JHC7 line. De-Comas et al.[4] report Brachyury expression in their cell line, but this expression decreases with serial passaging in vitro either due to epigenetic factors that influence its expression or perhaps because the cultured cell line from a xenograft is contaminated with a stromal Brachyury negative fraction that perhaps overpopulates the culture with serial passaging, therefore diluting the Brachyury-positive neoplastic fraction. All of our cells in culture express Brachyury as evidenced by colocalization of Brachyury and DAPI in JHC7 cells in all fields evaluated for immunostaining, making the likelihood of another cellular contaminant unlikely (Fig. 2a). In addition, injection of JHC7 cells into immunocompromised animals initiated tumors that remarkably resembled the parental tumor phenotype. Furthermore, we demonstrate for the first time that silencing of Brachyury using shRNA renders the morphology of chordoma cells to a more differentiated-like state, which leads to complete growth arrest with an inability to be passaged serially in vitro.

Consistent Brachyury expression is important when modeling chordoma in vitro and in vivo. Although the function of Brachyury in chordoma is unknown, there is evidence that this unique protein plays a critical role in tumor pathogenesis. Fernando and colleagues demonstrated that in the pancreatic tumor cell line PANC-1, overexpression of Brachyury induces changes characteristic of epithelial-to-mesenchymal transition, a critical step in cell migration, invasion, and metastasis.[5] Brachyury expression suppresses E-cadherin promoter activity and promotes Slug expression, which can influence tumor metastasis.[5] Interestingly,

an evaluation of lung tumor samples by the same group suggests that Brachyury mRNA was more commonly expressed in high-grade tumors than in low-grade tumors or normal lung tissue.[5] This work suggests that Brachyury may have a critical role in chordoma pathogenesis, and the JHC7 chordoma cell line and xenograft model uniquely allows for the evaluation of this important transcription factor.

Our work supports the possible role of Brachyury in promotion of a mesenchymal phenotype as evidenced by the gain of a more differentiated-like morphology with adherent stellate cells and decrease in the mesenchymal markers N-cadherin and Slug upon loss of Brachyury expression. A mesenchymal phenotype is associated with increased cell migration and invasion when Brachyury overexpression is forced in epithelial-derived cancers.[5] However, further research is warranted in understanding the possible role of Brachyury and epithelial-to-mesenchymal transition in chordomas. The JHC7 cell line provides an excellent model to explore this question.

The evidence that chordoma xenografts continue to resemble the parent tumor morphologically and histopathologically with continued expression of Brachyury with serial passaging in vitro and in xenografts offers some evidence that important pathophysiological pathways continue to be maintained. It is unclear if subcutaneous chordoma growth significantly alters the critical pathophysiological mechanisms of this tumor compared with intraosseous chordomas, but the slow growth rate in vivo is consistent with its slow growth rate clinically. Yet, an intraosseous model for human chordoma continues to be pursued. Collectively, these findings are consistent with and underscore the importance of recent advances that strongly implicate overexpression of Brachyury in the pathogenesis of chordoma.

Conclusions

The JHC7 cell line provides the first model system to study chordoma with Brachyury expression. We propose that Brachyury is a novel and attractive therapeutic target in the treatment of chordoma. Insight gained from the role of Brachyury expression in chordoma can facilitate our understanding of its role in other epithelial-derived cancers as well as in development. Furthermore, this model currently serves as a platform for the evaluation of several novel chemotherapeutic strategies to treat chordoma as it accurately recapitulates the disease.

Abbreviations used in this paper

DAB	3,3′-diaminobenzidine
DAPI	4,6′-diamino-2-phenylindole-dihydrochloride
DMEM/F12	Dulbecco modified Eagle medium/nutrient mixture F-12
FBS	fetal bovine serum
GAPDH	glyceraldehyde 3-phosphate dehydrogenase
HRP	horseradish peroxidase

| JHC7 | Johns Hopkins Chordoma line 7 |
MTT	3-(4,5-dimethylthiazol-2-yl)2,5-diphenyltetrazolium bromide
PBS	phosphate-buffered saline
PCR	polymerase chain reaction
shRNA	short hairpin RNA

References

1. Boriani S, Bandiera S, Biagini R, Bacchini P, Boriani L, Cappuccio M, et al. Chordoma of the mobile spine: fifty years of experience. Spine (Phila Pa 1976). 2006; 31:493–503. [PubMed: 16481964]

2. Casali PG, Messina A, Stacchiotti S, Tamborini E, Crippa F, Gronchi A, et al. Imatinib mesylate in chordoma. Cancer. 2004; 101:2086–2097. [PubMed: 15372471]

3. Choi KS, Cohn MJ, Harfe BD. Identification of nucleus pulposus precursor cells and notochordal remnants in the mouse: implications for disk degeneration and chordoma formation. Dev Dyn. 2008; 237:3953–3958. [PubMed: 19035356]

4. DeComas AM, Penfornis P, Harris MR, Meyer MS, Pochampally RR. Derivation and characterization of an extra-axial chordoma cell line (EACH-1) from a scapular tumor. J Bone Joint Surg Am. 2010; 92:1231–1240. [PubMed: 20439670]

5. Fernando RI, Litzinger M, Trono P, Hamilton DH, Schlom J, Palena C. The T-box transcription factor Brachyury promotes epithelial-mesenchymal transition in human tumor cells. J Clin Invest. 2010; 120:533–544. [PubMed: 20071775]

6. Fourney DR, Rhines LD, Hentschel SJ, Skibber JM, Wolinsky JP, Weber KL, et al. En bloc resection of primary sacral tumors: classification of surgical approaches and outcome. J Neurosurg Spine. 2005; 3:111–122. [PubMed: 16370300]

7. Gruneberg H. Genetical studies on the skeleton of the mouse. XXIII. The development of brachyury and anury. J Embryol Exp Morphol. 1958; 6:424–443. [PubMed: 13575656]

8. Hashimoto K, Fujimoto H, Nakatsuji N. An ECM substratum allows mouse mesodermal cells isolated from the primitive streak to exhibit motility similar to that inside the embryo and reveals a deficiency in the T/T mutant cells. Development. 1987; 100:587–598. [PubMed: 3327671]

9. Horten BC, Montague SR. In vitro characteristics of a sacrococcygeal chordoma maintained in tissue and organ culture systems. Acta Neuropathol. 1976; 35:13–25. [PubMed: 1274529]

10. Hsieh PC, Xu R, Sciubba DM, McGirt MJ, Nelson C, Witham TF, et al. Long-term clinical outcomes following en bloc resections for sacral chordomas and chondrosarcomas: a series of twenty consecutive patients. Spine (Phila Pa 1976). 2009; 34:2233–2239. [PubMed: 19752710]

11. Hsu W, Kosztowski TA, Zaidi HA, Dorsi M, Gokaslan ZL, Wolinsky JP. Multidisciplinary management of primary tumors of the vertebral column. Curr Treat Options Oncol. 2009; 10:107–125. [PubMed: 19548089]

12. Hsu W, Kosztowski TA, Zaidi HA, Gokaslan ZL, Wolinsky JP. Image-guided, endoscopic, transcervical resection of cervical chordoma. Technical note. J Neurosurg Spine. 2010; 12:431–435. [PubMed: 20367380]

13. McMaster ML, Goldstein AM, Bromley CM, Ishibe N, Parry DM. Chordoma: incidence and survival patterns in the United States, 1973–1995. Cancer Causes Control. 2001; 12:1–11. [PubMed: 11227920]

14. O'Donnell P, Tirabosco R, Vujovic S, Bartlett W, Briggs TW, Henderson S, et al. Diagnosing an extra-axial chordoma of the proximal tibia with the help of brachyury, a molecule required for notochordal differentiation. Skeletal Radiol. 2007; 36:59–65. [PubMed: 16810540]

15. Oakley GJ, Fuhrer K, Seethala RR. Brachyury, SOX-9, and podoplanin, new markers in the skull base chordoma vs chondrosarcoma differential: a tissue microarray-based comparative analysis. Mod Pathol. 2008; 21:1461–1469. [PubMed: 18820665]

16. Ostroumov E, Hunter CJ. The role of extracellular factors in human metastatic chordoma cell growth in vitro. Spine (Phila Pa 1976). 2007; 32:2957–2964. [PubMed: 18091487]

17. Palena C, Polev DE, Tsang KY, Fernando RI, Litzinger M, Krukovskaya LL, et al. The human T-box mesodermal transcription factor Brachyury is a candidate target for T-cell-mediated cancer immunotherapy. Clin Cancer Res. 2007; 13:2471–2478. [PubMed: 17438107]

18. Pereira BP, Zhou Y, Gupta A, Leong DT, Aung KZ, Ling L, et al. Runx2, p53, and pRB status as diagnostic parameters for deregulation of osteoblast growth and differentiation in a new pre-chemotherapeutic osteosarcoma cell line (OS1). J Cell Physiol. 2009; 221:778–788. [PubMed: 19746444]

19. Rashbass P, Cooke LA, Herrmann BG, Beddington RS. A cell autonomous function of Brachyury in T/T embryonic stem cell chimaeras. Nature. 1991; 353:348–351. [PubMed: 1922339]

20. Ricci-Vitiani L, Pierconti F, Falchetti ML, Petrucci G, Maira G, De Maria R, et al. Establishing tumor cell lines from aggressive telomerase-positive chordomas of the skull base. Technical note. J Neurosurg. 2006; 105:482–484. [PubMed: 16961149]

21. Salisbury JR. The pathology of the human notochord. J Pathol. 1993; 171:253–255. [PubMed: 8158454]

22. Salisbury JR, Deverell MH, Cookson MJ, Whimster WF. Three-dimensional reconstruction of human embryonic notochords: clue to the pathogenesis of chordoma. J Pathol. 1993; 171:59–62. [PubMed: 8229458]

23. Scheil S, Brüderlein S, Liehr T, Starke H, Herms J, Schulte M, et al. Genome-wide analysis of sixteen chordomas by comparative genomic hybridization and cytogenetics of the first human chordoma cell line, U-CH1. Genes Chromosomes Cancer. 2001; 32:203–211. [PubMed: 11579460]

24. Showell C, Binder O, Conlon FL. T-box genes in early embryogenesis. Dev Dyn. 2004; 229:201–218. [PubMed: 14699590]

25. Stacchiotti S, Marrari A, Tamborini E, Palassini E, Virdis E, Messina A, et al. Response to imatinib plus sirolimus in advanced chordoma. Ann Oncol. 2009; 20:1886–1894. [PubMed: 19570961]

26. Su Y, Luo X, He BC, Wang Y, Chen L, Zuo GW, et al. Establishment and characterization of a new highly metastatic human osteosarcoma cell line. Clin Exp Metastasis. 2009; 26:599–610. [PubMed: 19363654]

27. Tirabosco R, Mangham DC, Rosenberg AE, Vujovic S, Bousdras K, Pizzolitto S, et al. Brachyury expression in extra-axial skeletal and soft tissue chordomas: a marker that distinguishes chordoma from mixed tumor/myoepithelioma/parachordoma in soft tissue. Am J Surg Pathol. 2008; 32:572–580. [PubMed: 18301055]

28. Vormoor J, Baersch G, Decker S, Hotfilder M, Schäfer KL, Pelken L, et al. Establishment of an in vivo model for pediatric Ewing tumors by transplantation into NOD/scid mice. Pediatr Res. 2001; 49:332–341. [PubMed: 11228258]

29. Vujovic S, Henderson S, Presneau N, Odell E, Jacques TS, Tirabosco R, et al. Brachyury, a crucial regulator of notochordal development, is a novel biomarker for chordomas. J Pathol. 2006; 209:157–165. [PubMed: 16538613]

30. Wilson V, Beddington R. Expression of T protein in the primitive streak is necessary and sufficient for posterior mesoderm movement and somite differentiation. Dev Biol. 1997; 192:45–58. [PubMed: 9405096]

31. Yamaguchi T, Yamato M, Saotome K. First histologically confirmed case of a classic chordoma arising in a precursor benign notochordal lesion: differential diagnosis of benign and malignant notochordal lesions. Skeletal Radiol. 2002; 31:413–418. [PubMed: 12107574]

32. Yang C, Hornicek FJ, Wood KB, Schwab JH, Choy E, Iafrate J, et al. Characterization and analysis of human chordoma cell lines. Spine (Phila Pa 1976). 2010; 35:1257–1264. [PubMed: 20461036]

33. Yang C, Schwab JH, Schoenfeld AJ, Hornicek FJ, Wood KB, Nielsen GP, et al. A novel target for treatment of chordoma: signal transducers and activators of transcription 3. Mol Cancer Ther. 2009; 8:2597–2605. [PubMed: 19723879]

34. Yang XR, Ng D, Alcorta DA, Liebsch NJ, Sheridan E, Li S, et al. T (brachyury) gene duplication confers major susceptibility to familial chordoma. Nat Genet. 2009; 41:1176–1178. [PubMed: 19801981]

35. Yasuda T, Kanamori M, Nogami S, Hori T, Oya T, Suzuki K, et al. Establishment of a new human osteosarcoma cell line, UTOS-1: cytogenetic characterization by array comparative genomic hybridization. J Exp Clin Cancer Res. 2009; 28:26. [PubMed: 19239720]

36. York JE, Kaczaraj A, Abi-Said D, Fuller GN, Skibber JM, Janjan NA, et al. Sacral chordoma: 40-year experience at a major cancer center. Neurosurgery. 1999; 44:74–80. Manuscript submitted February 5, 2011. [PubMed: 9894966]
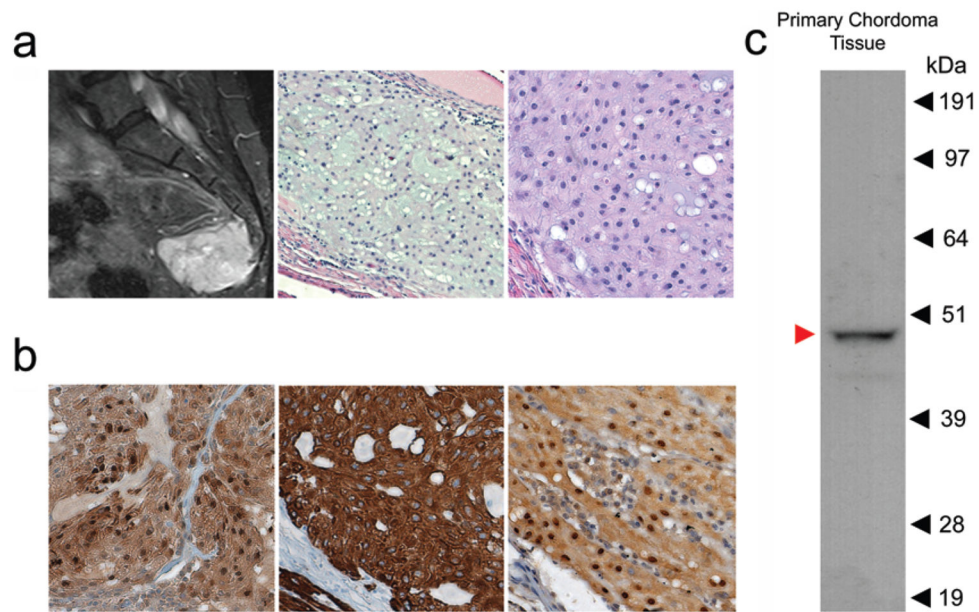
Fig. 1.
Images characterizing human chordoma tissue. **a:** Sagittal T1-weighted MR image **(left)** showing sacral chordoma tissue. Photomicrographs **(center and right)** showing intraoperatively obtained sacral chordoma tissue with physaliferous phenotype. H & E, original magnification × 10 **(center)**, × 20 **(right). b:** Photomicrographs showing chordoma tissue positive for S100β **(left)**, cytokeratin **(center)**, and Brachyury (immunohistochemistry; **right**). Stained with DAB, original magnification × 20. **c:** Western blot showing expression of Brachyury protein in primary sacral chordoma sample at 49 kD (*red arrow*).
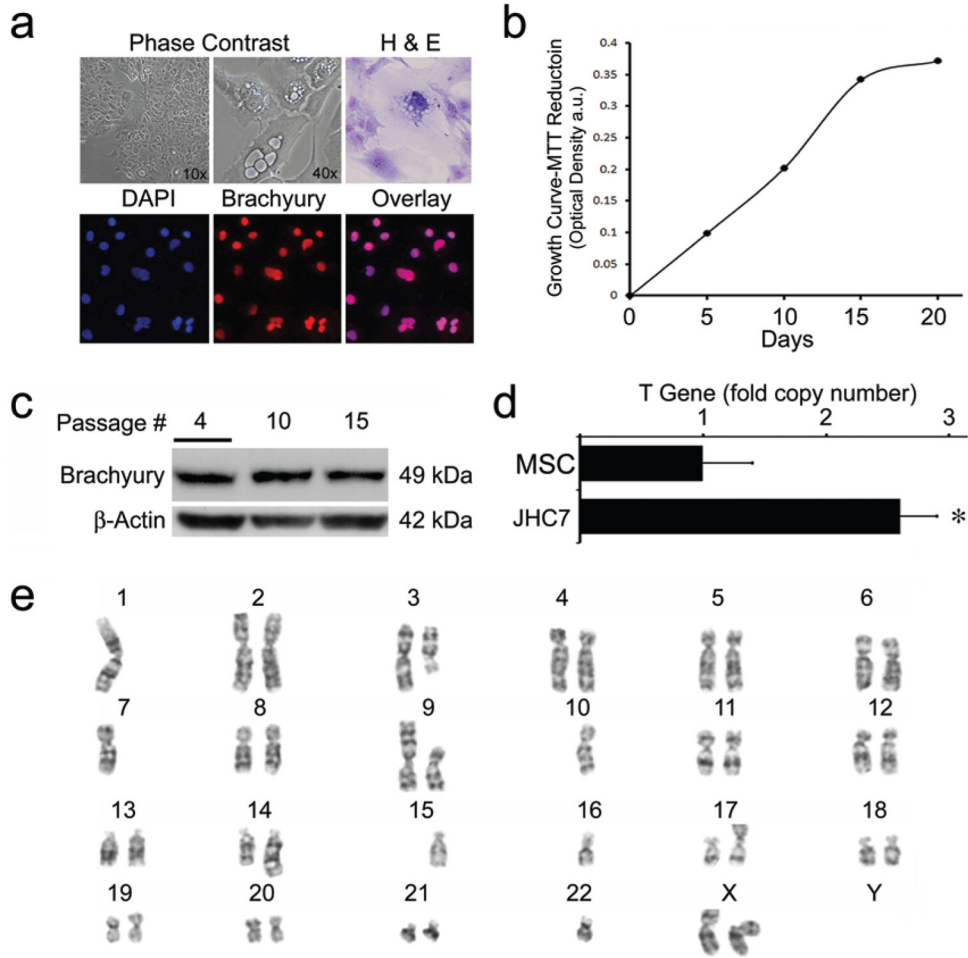
Fig. 2.
Establishment and characterization of human sacral chordoma-derived cell lines. **a:** Cultured chordoma cells (JHC7) display physaliferous features in phase-contrast images **(left and center)** and after staining with H & E **(right)**. Original magnification × 10 **(left and right)**, × 40 **(center)**. Nuclear localization of Brachyury expression overlaps with DAPI signal, which counterstains nuclei in overlay images (immunocytochemistry). Original magnification × 20. **b:** Graph of JHC7 cell growth in vitro (using the MTT assay) demonstrates a doubling time of approximately 5 days. a.u. = arbitrary units. **c:** Western blot showing Brachyury expression in JHC7 cells harvested from the 4th, 10th, and 15th passages. Immunoreactive bands for Brachyury were prominent at 49 kD, and β-actin expression was probed for equal loading. **d:** Graph of *T* gene locus gain in JHC7 cells as demonstrated by an approximately 2-fold change in *T* gene copy number when compared with human mesenchymal stem cells (MSC). The GAPDH gene served as loading control using DNA PCR. *p < 0.05. **e:** One representative metaphase for karyotype analysis of G-banded chromosomes identified numerical, structural, and clonal abnormalities in JHC7 cells (for detailed description of analysis, see *Results*).
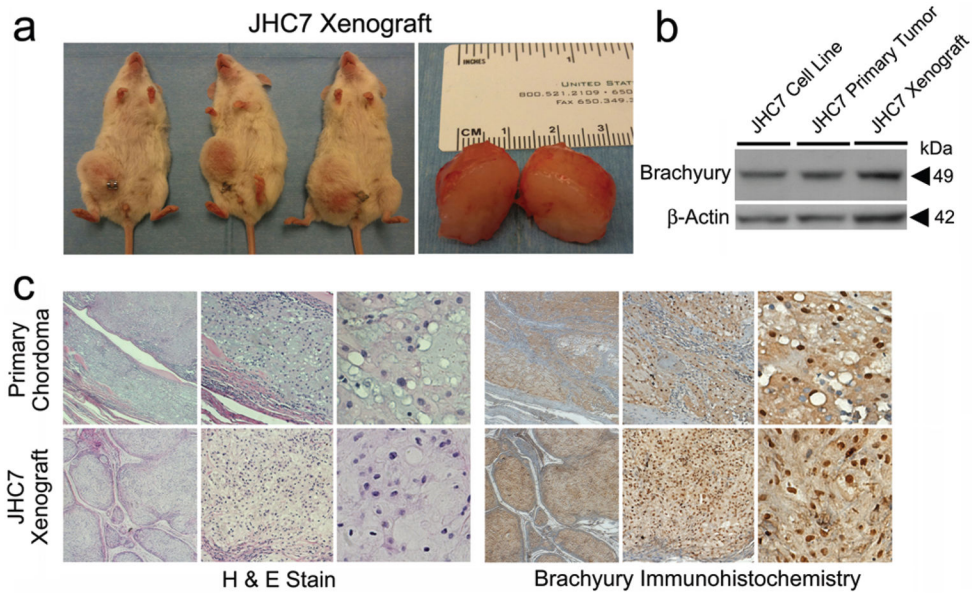
Fig. 3.
Subcutaneous injection of established chordoma cells results in tumor that recapitulates the parental tumor phenotype. **a:** Mice injected with 2 million, 1 million, and 500,000 chordoma cells formed tumors within 3–4 months after implantation at the initial site of injection and grossly resembled parental tumor. Tumors pictured were obtained 6 months after injection. **b:** In a Western blot analysis of the JHC7 chordoma cell line, the original parental tumor (JHC7 Primary Tumor) and chordoma xenograft revealed prominent expression of Brachyury at 49 kD. **c:** Xenografts revealed a lobulated tumor composed of cells separated by fibrous septa, resembling the parent tumor (JHC7 Primary Tumor/Primary Chordoma). These tumors possessed physaliferous features characteristic of chordoma (H & E). Cells in the xenograft and parental tumor expressed Brachyury that localized to the nucleus (immunohistochemistry). Original magnifications × 4 **(first and fourth columns)**, × 10 **(second and fifth columns)**, and × 40 **(third and sixth columns)**.
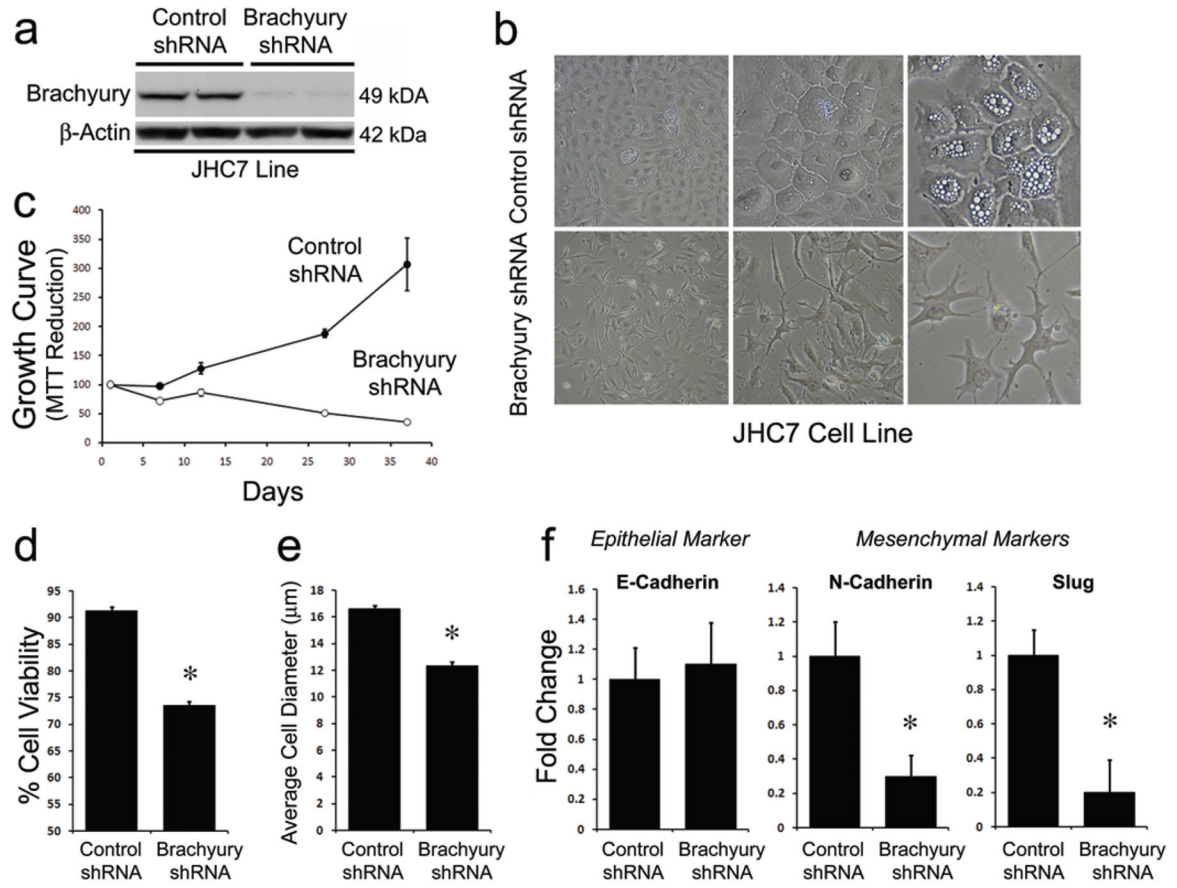
Fig. 4.

Loss of Brachyury leads to phenotypic changes and loss of proliferation. **a:** Western blot analysis showing production of Brachyury-knockdown JHC7 cells using shRNA confirmed by loss of Brachyury expression. **b:** Phase-contrast images of Brachyury-knockdown JHC7 cells exhibiting a loss of physaliferous features and exhibiting a more differentiated-like phenotype with stellate-appearing cells. Original magnification × 10 (**left column**), × 20 (**center column**), and × 40 (**right column**). **c:** Using an MTT assay, complete loss of proliferation (p < 0.05) is observed in Brachyury knockdown JHC7 cells (Brachyury shRNA) when compared with JHC7 cells with empty vector (control shRNA). **d:** Using trypan blue exclusion, JHC7 cell viability 20 days after Brachyury knockdown is compared with control shRNA. *p < 0.05. **e:** Average JHC7 cell diameter of Brachyury shRNA compared with control shRNA cells. *p < 0.05. **f:** Changes in epithelial and mesenchymal markers in JHC7 cells 10 days after Brachyury knockdown (quantitative reverse transcriptase PCR); only changes in mesenchymal markers were significant (*p < 0.05).